of ordinary differential equations. We indicated how the particular relation selected for discretization of the derivatives in the process model influences the accuracy of the estimates of the coefficients. It is quite possible for one discretization method to yield highly biased estimates if the equations are stiff whereas selection of another method and/or time interval for taking measurements would yield quite satisfactory results. Based on the examples used here, one can apply the guidelines of error evaluation to various other kinetic models that may or may not be linear in the coefficients.

NOTATION

a,b = coefficients in integration (discretization) formula
A = process coefficient matrix
D = complex domain for integration in a cost function
e = observation noise
$\underline{f}$ = process function vector
F = parameter free matrix of process
h = integration (discretization) time step and sampling interval
J_o,J_1 = cost function to obtain an optimal discretization relation
k = discrete time variable
k_1,k_2 = kinetic parameters
L = discretization relation
m = number of unknown parameters
n = number of state variables
$\underline{p}$ = vector of unknown process parameters
p = unknown process parameter
q,r = step number of integration (discretization)
r_1,r_2 = rate of first and second reactions
R = region in which relative error of apparent characteristic roots is less than a specified value
t = time variable
T = process diagonalization matrix
$\underline{x}$ = state vector
$\underline{y}$ = measurement vector
z = state variable of the diagonalized process
$\epsilon_{\lambda h}$ = relative error of the apparent characteristic root
λ = characteristic root of process
$\overline{\lambda}$ = apparent characteristic root
$\hat{}$ = estimate

LITERATURE CITED

Box, G. E. P., and G. M. Jenkins, *Time Series Analysis: Forecasting and Control*, Holden-Day, San Francisco (1976).
Froment, G. F., "Model Discrimination and Parameter Estimation in Heterogeneous Catalysis," *AIChE J.*, **21**, 1041 (1975).
Glowinski, J., and J. Stocki, "Estimation of Kinetic Parameters—Initial Guess Generation Method," *AIChE J.*, **27**, 1041 (1981).
Himmelblau, D. M., C. R. Jones, and K. B. Bischoff, "Determination of Rate Constants for Complex Kinetics Model," *Ind. Eng. Chem. Fund.*, **6**, 539 (1967).
Himmelblau, D. M., *Fault Detection and Diagnosis in Chemical and Petrochemical Processes*, Elsevier Scientific Publishing Co., New York (1978).
Jazwinski, A. H., *Stochastic Processes and Filtering Theory*, Academic Press, New York (1970).
Landau, Y. D., *Adaptive Control, The Model Reference Approach*, Marcel Dekker Inc., New York (1979).
Luke, Y. L., *The Special Functions and Their Approximation*, Academic Press, New York (1969).
Pexidr, V., "Estimation of Nonlinear-Regression Kinetic Data III. Evaluation of Integral Kinetic Data," *Chem. Prum.*, **24**, 254 (1974).
Seinfeld, J. H., "Nonlinear Estimation Theory," *Ind. Eng. Chem.*, **62**, 32 (1970).
Seinfeld, J. H., and G. H. Gavalas, "Analysis of Kinetic Parameters from Batch and Integral Reaction Experiments," *AIChE J.*, **16**, 644 (1970).
Watanabe, K., and H. Shimizu, "Parameter Optimization Software Using Padé's Computation of Transient Response," *Electrical Eng. in Japan*, **95**, 119 (1975).

Manuscript received March 1, 1982; revision received October 5, and accepted October 20, 1982.

Moving Boundary Problems in Simple Shapes Solved by Isotherm Migration

The Modified Isotherm Migration Method (MIMM) is developed for solving one-dimensional Stefan-type problems of multifront propagation in slabs, cylinders and spheres with a boundary condition of the third kind (radiation-type boundary condition). The method is illustrated for all three geometries with applications to the thawing of ice and to the freezing of a 50–50 dispersion of tetradecane in water, a system in which two freezing fronts propagate simultaneously.

Y. TALMON
Department of Chemical Engineering
Technion—Israel Institute of Technology
Haifa, Israel 32000
and
H. T. DAVIS and
L. E. SCRIVEN
Department of Chemical Engineering
and Materials Science
University of Minnesota
Minneapolis, MN 55455

SCOPE

Classical analytical solutions have been found to just a few simple cases of moving boundary problems. Although modern analysis by computer-aided finite element methods is now showing great promise (Comini et al., 1974; Bonnerot and Jamet, 1977), most numerical solutions have been based on the finite difference approximation. One such scheme suitable especially

for one-dimensional moving front methods is the Isotherm Migration Method (IMM) first proposed by Chernous'ko (1970) and Dix and Cizek (1971). In this method one tracks in time t, the movement of a given set of isotherms, u_i, including any phase transformation front. Thus the distance x becomes the dependent variable instead of the temperature. IMM can be extended to two dimensions as was shown by Crank and Gupta (1975); but as pointed out by Shamsundar (1978), it is faced with difficulty when the boundary temperature is not fixed such as in the case of a boundary condition of the third kind (known also as a radiation-type boundary condition or as a Robin boundary condition).

In a recent paper (Talmon et al., 1981), we described the Modified Isotherm Migration Method (MIMM) which can be applied when there is more than one moving phase-transformation front and when there are external surface resistances. The MIMM, originally suggested for one-dimensional problems with unidirectional heat flux, is here generalized to handle one-dimensional problems with radial heat flux, as in the simple shapes of the cylinder and the sphere.

CONCLUSIONS AND SIGNIFICANCE

The generalized form of the Modified Isotherm Migration Method presented here can be used to advantage to solve one-dimensional Stefan-type problems of multifront propagation in a slab, a cylinder, or a sphere with a radiation-type boundary condition. Use of the MIMM in its generalized form is demonstrated for problems of freezing and thawing single-component and two-component systems. The method can be used to solve any other one-dimensional problem that involves moving fronts of constant temperature. Practical situations where these methods can be used are numerous: examples include manufacturing processes based on solidification, casting and molding, solid-solid phase transitions, freezing and thawing of soil and lakes, and food processes such as freezing, thawing, drying and cooking. Applications of MIMM to the problem of freezing and thawing of meat are discussed by Talmon and Davis (1981) and to the problem of heating frozen foods by Talmon et al. (1982).

PHYSICAL MODEL

A long slab of thickness 2a, a long cylinder of diameter 2a, or a sphere of diameter 2a with a given initial temperature profile, u_o, is immersed at $t = 0$ in a fluid of temperature u_a. Conditions are symmetrical so that temperature depends on just one position coordinate, x (Figure 1). As the body cools or heats the temperature of its surface at some time reaches a phase-change temperature and a phase-boundary begins to move towards the center. In a homogeneous material that undergoes more than one phase change in the temperature interval, or in a dispersion of more than one phase, more than one moving front of phase change traverses the distance between the surface and the center. The fronts demarcate distinct regions, each having different physical properties.

To illustrate we imagine the cross-section (Figure 2) of a cylindrical sample of a liquid-liquid dispersion. As the sample is frozen, three regions can be distinguished: region 1, a solid-solid dispersion; region 2, a solid-liquid dispersion; and region 3, a liquid-liquid dispersion. The front f_1 separates regions 1 and 2 and the front f_2 separates region 2 and 3. Eventually f_2 will reach the centerline (center plane in a slab, center in a sphere) leaving only regions 1 and 2 in the sample. Solidification will be completed when f_1 reaches the centerline.

In our model we neglect density changes with changes of phase, and we assume that the thermal properties of each region are set by its composition and physical state alone and are not temperature-dependent. We suppose the heat flux between the sample and the ambient fluid is adequately described by a heat transfer coefficient $h(u)$. If the sample is contained by a wall or shell, our analysis can still be used if a quasisteady-state approximation holds within the walls, in which case an effective h can be calculated.

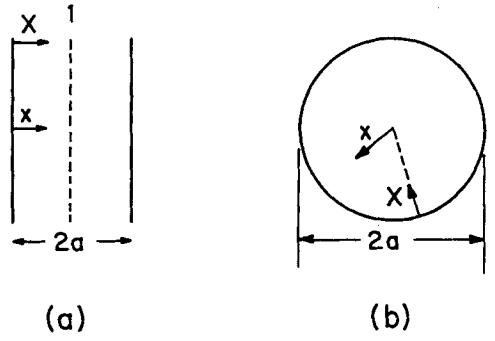

Figure 1. Cross section of a slab (a) and a cylinder or a sphere (b).

MODIFIED ISOTHERM MIGRATION METHOD

The mathematical model of the case of a long slab and a detailed description of the Modified Isotherm Migration Method were given earlier by Talmon et al. (1981). We present here only the main governing equations that need generalization to cover the cases of the long cylinder and the sphere and some useful details not put in the earlier paper.

In each region j demarcated by a front or fronts, the temperature u_j must satisfy the heat conduction equation:

$$\frac{1}{\kappa_j}\frac{\partial u_j}{\partial t} = \frac{f-1}{x}\frac{\partial u_j}{\partial x} + \frac{\partial^2 u_j}{\partial x^2} \tag{1}$$

where κ_j is the thermal diffusivity of region j, and f, the "form factor," is

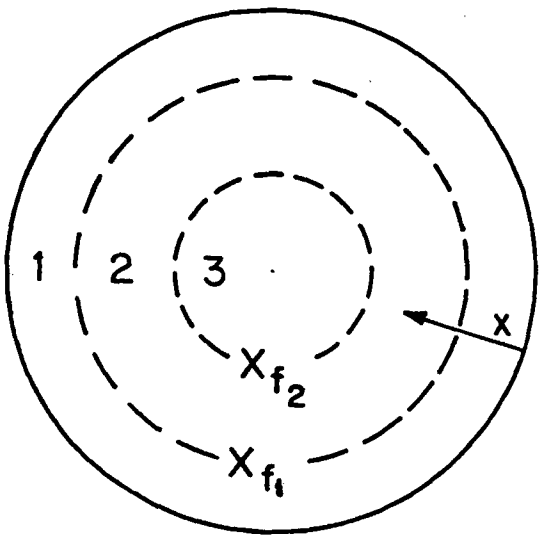

Figure 2. Model of freezing (thawing) cylinder or sphere with two moving fronts, at X_{f1} and X_{f2} separating three distinct regions: e.g., 1—solid-solid dispersion, 2—solid-liquid dispersion, 3—liquid-liquid dispersion.

$$f = \begin{cases} 1, \text{ slab} \\ 2, \text{ cylinder} \\ 3, \text{ sphere} \end{cases} \tag{2}$$

Dimensionless variables are appropriate:

$$X \equiv \begin{cases} \dfrac{x}{a}, & f = 1 \\ \dfrac{a-x}{a}, & f = 2,3 \end{cases} \tag{3}$$

$$T \equiv \frac{\kappa_1 t}{a^2}, \quad \alpha_j \equiv \frac{\kappa_j}{\kappa_1}, \quad \beta_j \equiv \frac{K_{j+1}}{K_j}, \quad H_j \equiv \frac{ha}{K_j} \tag{4}$$

Here K_j is the thermal conductivity of region j. Now we can write Eq. 1 as

$$\frac{1}{\alpha_j}\frac{\partial u_j}{\partial T} = \frac{(f-1)}{1-X}\frac{\partial u_j}{\partial X} + \frac{\partial^2 u_j}{\partial X} \tag{5}$$

The equation of energy flux balance governs the movement of front f_j:

$$\frac{\partial u_j}{\partial X} - \beta_j \frac{\partial u_{j+1}}{\partial X} = S_j \frac{dX_{fj}}{dT}, \quad \text{at } X = X_{fj} \tag{6}$$

where X_{fj} denotes the dimensionless position of f_j. S_j is a reduced latent heat in degrees associated with the front f_j:

$$S_j \equiv \frac{\rho \phi_j \ell_j \kappa_1}{K_j} \tag{7}$$

where ϕ_j is the volume fraction of the component that undergoes a phase change at f_j with a latent heat of ℓ_j, and ρ is the mean density of the system. The boundary conditions at $X = 0$, $X = 1$ and at the moving fronts are

$$H_j[u_j(0,T) - u_a] = \left.\frac{\partial u_j}{\partial X}\right|_{X=0} \tag{8}$$

$$\left.\frac{\partial u_j}{\partial X}\right|_{X=1} = 0 \tag{9}$$

$$u_j(X_{fj},T) = u_{j+1}(X_{fj},T) = u_{fj} \tag{10}$$

The initial condition is

$$u(X,0) = u_o \tag{11}$$

For the MIMM we rewrite Eqs. 5 and 7 so that X is expressed as a function of u and T:

$$\frac{\partial X}{\partial T} = \frac{\alpha_j(f-1)}{1-X} + \alpha_j \frac{\partial^2 X}{\partial u_j^2}\left(\frac{\partial X}{\partial u_j}\right)^{-2} \tag{12}$$

$$S_j \frac{\partial X_{fj}}{\partial T} = \left(\frac{\partial X}{\partial u_j}\right)^{-1} - \beta_j \left(\frac{\partial X}{\partial u_{j+1}}\right)^{-1}, \quad X = X_{fj} \tag{13}$$

The use of the boundary and initial conditions in this form is obvious. Three-point centered finite difference approximations for the derivatives in Eqs. 12 and 13 give:

$$X_i^{n+1} = X_i^n + \alpha_j \Delta T^n \left[4\frac{X_{i+1}^n - 2X_i^n + X_{i-1}^n}{(X_{i+1}^n - X_{i-1}^n)^2} + \frac{f-1}{1-X_i^n}\right] \tag{14}$$

$$X_{fj}^{\eta+1} = X_{fj}^{\eta} + \frac{\Delta T^n}{S_j}\left[\frac{\Delta u_j}{X_{fj}^{\eta} - X_{fj-1}^{\eta}} - \frac{\beta_j \Delta u_{j+1}}{X_{fj+1}^{\eta} - X_{fj}^{\eta}}\right] \tag{15}$$

X_{fj-1} and X_{fj+1} denote positions of the isotherms on either side of the front at X_{fj}, ΔT^n is the time step determined by the isotherms X_i^n and Δu_j is the temperature difference between isotherms in region j.

For $f = 2$ (cylinder) and $f = 3$ (sphere) we have at $X = 1$, in addition to Eq. 9, the following requirement from radial symmetry:

$$\lim_{X\to 1} \frac{1}{1-X}\frac{\partial u_j}{\partial X} = \frac{\partial^2 u_j}{\partial X^2} \tag{16}$$

Combined with Eq. 5 this gives the condition

$$\frac{\partial u}{\partial T} = f\alpha_j \frac{\partial^2 u_j}{\partial X^2} \quad \text{at } X = 1 \tag{17}$$

Equation 17 is, of course, valid also for $f = 1$. We combine Eq. 17 with the symmetry boundary condition (Eq. 9) to write a five-point centered finite difference approximation for the second derivative, an approximation which yields an expression for u_c, the temperature at the center:

$$u_c^{n+1} = u_c^n + 2f\alpha_j \Delta T^n \frac{-p^4 u_{m-1}^n + q^4 u_m^n - (q^4 - p^4)u_c^n}{q^4 p^2 - q^2 p^4} \tag{18}$$

Here m denotes the isotherm closest to $X = 1$, and

$$q \equiv 1 - X_{m-1}, \quad p \equiv 1 - X_m \tag{19}$$

When $p \to 0$, i.e., when X_m approaches $X = 1$, Eq. 18 becomes

$$u_c^{n+1} = u_c^n + 2f\alpha_j \Delta T^n \frac{u_m^n - u_c^n}{p^2} \tag{20}$$

It is appropriate to insure that $u_c^{n+1} > u_m^n$ in cooling, or the opposite in heating, and so we impose the following restriction on ΔT:

$$\Delta T^n < \frac{p^2}{2f\alpha_j} \tag{21}$$

An additional stability criterion arises from Eq. 14. It is a modification of Dix and Cizek's (1971) original criterion:

$$\Delta T^n < \alpha_j \left[\frac{8}{(X_{i+1}^n - X_{i-1}^n)^2} - \frac{f-1}{X_i^n(1-X_i^n)}\right]^{-1} \tag{22}$$

Their criterion, which is equivalent to setting $f = 1$, is more conservative and can be used for $f = 2$ and $f = 3$ too.

The equation governing the movement of u_m, the isotherm closest to $X = 1$, must also be modified to account for the first term on the righthand side of Eq. 5; it becomes:

$$X_m^{n+1} = X_m^n + \alpha_j \Delta T^n \times \left\{\frac{2(yz^2 + zy^2)[z - (y+z)X_m^n + yX_{m-1}^n]}{[z^2 - (z^2 - y^2)X_m^n - y^2 X_{m-1}^n]^2} + \frac{f-1}{1-X_m^n}\right\} \tag{23}$$

where

$$y \equiv u(1,T) - u_m \quad \text{and} \quad z \equiv u_m - u_{m-1} \tag{24}$$

The isotherm at $X = 0$ is advanced by the following finite difference equation based on forward three point approximations to the derivatives in Eq. 12:

$$X_1^{n+1} = \alpha_j \Delta T^n \left[4\frac{-2X_2^n + X_3^n}{(4X_2^n - X_3^n)^2} + (f-1)\right] \tag{25}$$

Equations 14, 15, and 18–22 can replace the corresponding equations of Talmon et al. (1981), and the procedure described there can thus be used for solving IMM and MIMM problems not only in long slabs but also in long cylinders and in spheres, provided conditions are radially symmetric.

RESULTS

Figure 3 shows temperature profiles calculated for the thawing of an ice sample, initially at its melting point, by suddenly raising the temperature at $X = 0$ to 10°C. The IMM was used with two generalizations of the present paper. Figure 3a shows the case of the slab. The initial profile (for $T = 0.05$) was calculated by the analytic solution which is available for this case. That solution is identical to the one for the semiinfinite slab (in the x-direction) until the thawing front reaches $X = 1$. The data used for all our calculations are given in Table 1.

Figures 3b and 3c show temperature profiles at several dimensionless times in a cylinder and in a sphere under the same conditions as in Figure 3a. The initial profiles for these cases were calculated by the analytic solution available for the slab case. Its use is justified by the short length of penetration ($X_f = 0.06$) for the

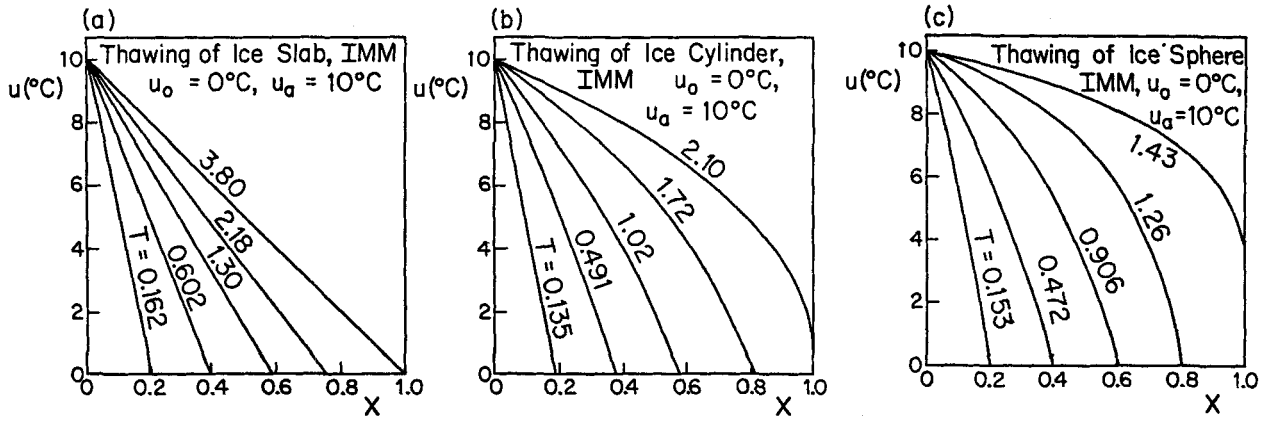

Figure 3. Thawing ice initially at its melting point by suddenly raising its surface temperature to 10°C: (a) a slab (b) a cylinder (c) a sphere.

TABLE 1. DATA FOR THE SAMPLE CALCULATIONS OF FIGURES 3, 4, AND 5

	Fig. 3	Fig. 4	Fig. 5
H_1 (≡ Bi)	—	1.86	0.242
S_1 (°C)	73.6	73.6	233
S_2 (°C)	—	—	53.4
u_o (°C)	0	0	22
u_a (°C)	10	10	−10
u_{f1} (°C)	0	0	0
u_{f2} (°C)	—	—	6
$K_1 \times 10^2$ (W/m·K)	5.52	5.52	1.44
$K_2 \times 10^2$ (W/m·K)	—	1.50	6.44
$K_3 \times 10^2$ (W/m·K)	—	—	2.99
$\kappa_1 \times 10^7$ (m²/s)	1.44	1.44	9.00
$\kappa_2 \times 10^7$ (m²/s)	—	—	2.35
$\kappa_3 \times 10^7$ (m²/s)	—	—	1.07
α_2	—	—	0.261
α_3	—	—	0.119
β_1	—	0.271	0.446
β_2	—	—	0.465

time selected (T = 0.05). The most striking feature is the curvature of the profiles; their second derivatives are negative in contrast to the slightly positive second derivatives of Figure 3a. The profiles steepen as the moving front approaches X = 1. For a given X_f they are steeper in the sphere. Similar profiles were reported by Riley et al. (1974). As expected, the time for complete thawing goes down with increasing f; i.e., the sphere thaws more quickly than the cylinder which thaws more quickly than the slab of half thickness equal to its radius.

Figure 4 shows profiles calculated by the generalized MIMM for the case of an ice sample, initially at its melting point, which was suddenly immersed in a fluid of bulk temperature 10°C. The heat transfer coefficient between the fluid and the sample was taken as 113 W/m²·K (20 Btu/h·ft²·°F). For a = 0.01 m, the Biot number ($Bi \equiv ha/K$) equals 1.86. No initial profile is needed for this case; the MIMM can handle the calculation from T = 0.

Figure 4a shows that temperature profiles in the slab have slightly positive second derivatives. The temperature at X = 0 is not constant and increases as the front nears X = 1. Figures 4b and 4c show the temperature profiles for the long cylinder and the sphere. The negative second derivatives are as pronounced as in Figure 3. The time needed for complete freezing gets shorter; at the completion of thawing, the temperature at X = 0 grows higher in the progression, slab, cylinder and sphere.

In Figure 5 we demonstrate the use of the MIMM for calculating temperature profiles in the freezing of a liquid-liquid dispersion. The example is tetradecane in water, with 1:1 weight ratio. The sample—a slab, a long cylinder or a sphere—initially at room temperature (22°C) is suddenly immersed in a coolant at −10°C. The heat transfer coefficient between the sample and the bulk fluid is taken to be 113 W/m²·K (20 Btu/h·ft²·°F). The initial profile, at the instant when the temperature at X = 0 reaches the first point of change of phase, is calculated for the slab (Figure 5a) and for the cylinder (Figure 5b) from published analytical solutions expressed as infinite series; for the sphere (Figure 5c) the use of available charts (e.g., those of Welty et al., 1969) was found to be more practical.

The first three profiles of Figure 5a show the propagation of the freezing front of tetradecane. The temperature profile near X = 1 becomes practically flat at 6° (T = 30.61), and solidification of tetradecane is complete at T = 31.20. At T = 31.84, the water freezing front appears. The temperature profile near X = 1 becomes practically flat at T = 131.6, and complete solidification occurs at T = 159.9.

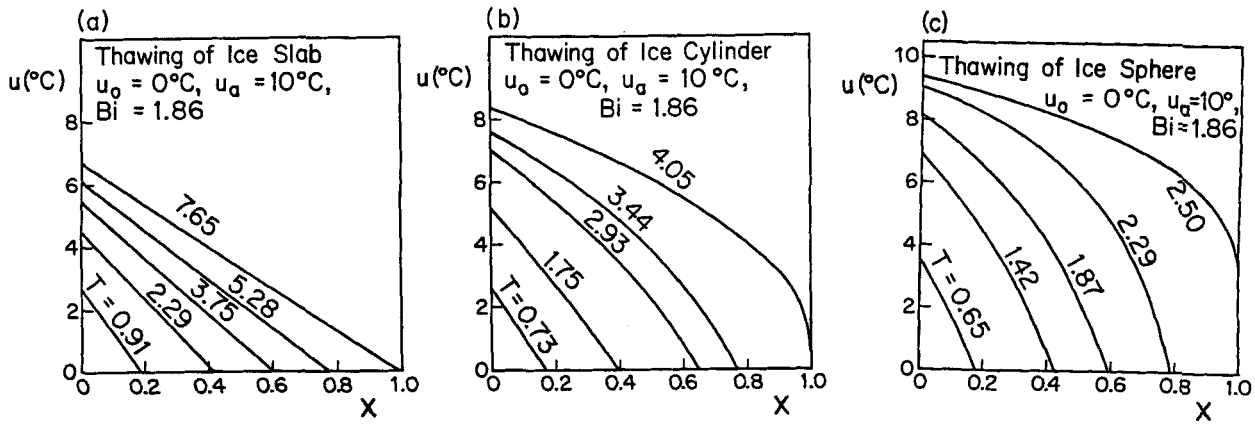

Figure 4. Thawing ice initially at its melting point by suddenly placing it in a fluid at 10°C with a heat transfer coefficient of h = 113 W/m²·K (20 Btu/ft²·h·°F): (a) a slab (b) a cylinder (c) a sphere.

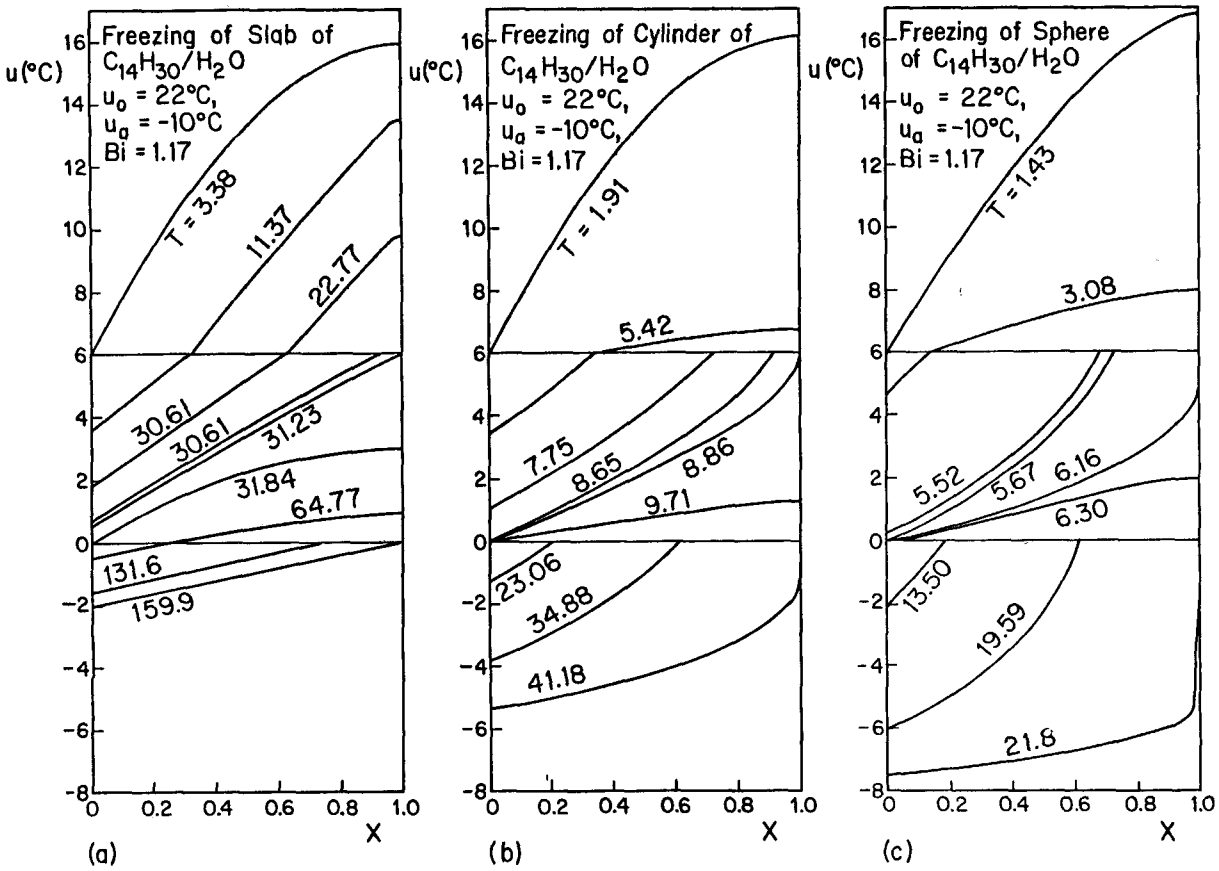

Figure 5. Freezing a 1:1 tetradecane-in-water dispersion by suddenly placing it in a fluid at −10°C. Tetradecane freezes at 6°C, water at 0°C. A heat transfer coefficient of h = 113 W/m²-K was taken between the surface and the fluid: (a) a slab (b) a cylinder (c) a sphere.

In the cylinder (Figure 5b) the profile between the first front and $X = 1$ becomes practically flat at $T = 7.75$, and before the first front disappears, the second enters at $T = 8.65$. The movement of the water freezing front is at first very slow, as is evident from the figure. After the flattening of the profile near $X = 1$, the situation becomes similar to that of Figure 4 and the second derivative of the profiles changes sign.

The profiles in the sphere (Figure 5c) are qualitatively similar to those in the cylinder (Figure 5b) but tend to be steeper near $X = 1$. As in the single front case of Figure 4, complete freezing (thawing) takes a shorter time for larger f, and the surface temperature at complete freezing gets closer to the ambient temperature.

ACKNOWLEDGMENTS

This work was supported by grants from the Department of Energy and the Computer Center of the University of Minnesota.

LITERATURE CITED

Bonnerot, R., and J. Jamet, "Numerical Computation of the Free Boundary for the Two-Dimensional Stefan Problem by Space-Time Finite Elements," *J. Comp. Phys.*, **25**, 163 (1977).

Chernous'ko, F. L., "Solution of Non-Linear Heat Conduction Problems in Media with Phase Change," *Int. Chem. Eng.*, **10**, 42 (1970).

Comini, J., S. Del Guidice, R. W. Lewis, and D. C. Zienkiewicz, "Finite Element Solution of Non-Linear Heat Conduction Problems with Special Reference to Phase Change," *Int. J. Num. Meth. Eng.*, **8**, 613 (1974).

Crank, J., and R. S. Gupta, "Isotherm Migration in Two Dimensions," *Int. J. Heat Mass Transfer*, **18**, 1101 (1975).

Dix, R. C., and J. Cizek, "The Isotherm Migration Method for Transient Heat Conduction Analysis," Proc. Fourth Int. Heat Transfer Conf., **1**, Paris, ASME (1971).

Riley, D. S., F. T. Smith, and G. Poots, "The Inward Solidification of Spheres and Circular Cylinders," *Int. J. Heat Mass Transfer*, **17**, 1507 (1974).

Shamsunder, N., "Comparison of Numerical Methods for Diffusion Problems with Moving Boundaries," *Moving Boundary Problems*, D. G. Wilson, A. D. Solomon, and P. T. Boggs, Eds., 165, Academic Press, New York (1978).

Talmon, Y., H. T. Davis, and L. E. Scriven, "Progressive Freezing of Composites Analyzed by Isotherm Migration Method," *AIChE J.*, **27**, 928 (1981).

Talmon, Y., and H. T. Davis, "Analysis of Propagation of Freezing and Thawing Fronts," *J. Food Sci.*, **46**, 1478 (1981).

Talmon, Y., E. A. Davis, J. Gordon, and H. T. Davis, "Temperature Profiles in Heated Frozen Foods," *AIChE Symp. Ser.* Vol. 78, No. 218, pages 76–82 (1982).

Welty, J. R., C. E. Wicks, and R. E. Wilson, "Fundamentals of Momentum, Heat and Mass Transfer," 635, John Wiley, New York (1969).

Manuscript received July 6, 1982; revision received November 8, and accepted December 14, 1982.

NOTATION

a = half width of slab, radius of cylinder or sphere
Bi = Biot number, ha/K
f = "form factor," 1 for slab, 2 for cylinder, 3 for sphere
f_j = jth moving front of phase change
h = heat transfer coefficient
H_j = dimensionless heat transfer coefficient, ah/K_j ($\equiv Bi$)
K = thermal conductivity
ℓ = latent heat of phase change
p = distance of last isotherm to the center
q = distance of the isotherm before last to the center
S_j = reduced latent heat of change of phase (degrees)
t = time
T = dimensionless time, a^2t/k_1
u = temperature

x = distance
X = dimensionless distance, x/a or $(a - x)/a$
y = temperature difference defined by Eq. 24
z = temperature difference defined by Eq. 24

Greek Letters

$\alpha_j = \kappa_j/\kappa_1$
$\beta_j = K_{j+1}/K_j$
κ = thermal diffusivity
ρ = average density of the system
ϕ = volume fraction

Subscripts

o = initial
a = ambient
c = at the center
fj = jth moving front of phase change
i = ith isotherm
j = jth region
m = isotherm closest to $X = 1$

Superscripts

n = nth time step

Kinetics of the Approach to Sorptional Equilibrium by a Foodstuff

G. N. ROMAN, M. J. URBICAIN, and ENRIQUE ROTSTEIN

Planiqui (Uns-Conicet)
Bahia Blanca, Argentina

The kinetics of equilibration of a vegetable foodstuff with moist air are studied on the basis of its cellular structure. The problem is modelled as a coupled heat and mass transfer phenomenon; since there is a significant shrinkage as moisture decreases, the model takes the effect into account by changing the basis for the mass and energy balances. The resulting nonlinear second-order partial differencial equations are solved numerically; predicted values of moisture decrease and temperature gain with time are compared with experimental data. A sensitivity analysis of the solution to values of the transport properties shows that the value of effective diffusivity and heat and mass transfer coefficient may alter significantly the predicted equilibration kinetics and center temperature. The adopted value for heat of sorption has less influence. Changes in effective thermal conductivity and porosity bear little influence on predictions.

SCOPE

Many practical design problems, such as dehydration, packaging and storage, arise when a foodstuff is removed from an equilibrium situation and is required to attain a new one. Much attention has been given to experimental determinations and theoretical predictions of the equilibrium values for the system moist air–foodstuff. The latter were based on adapting theoretical expressions developed for the sorption of gas molecules on nonvolatile solid surfaces or were empirical correlations (Labuza, 1974). An alternative approach was to recognize the actual cellular tissue structure of the foodstuff and to develop a predictive equation on the basis of equal chemical potential at the intervening phases (Rotstein and Cornish, 1978b).

Much less attention has been given to the kinetics of the phenomenon by which equilibration is attained (Román et al., 1979), although the subject is of interest because of many practical situations in packaging as well as in storing, be it cold, room temperature or controlled atmosphere conservation. In such cases it is required to model the kinetics to approach the problem in a sound engineering fashion. If the understanding of the kinetics is based on recognizing the actual cellular tissue structure of the foodstuff, it has the potential of providing useful insight as to the relationship between structure and behavior. In addition, the parallel between the situation of moisture equilibration and drying provides insight useful for the latter process.

In this paper, a model is built on the basis of the cellular structure of a typical fruit and the fact that moisture equilibration is a coupled heat and mass transfer phenomenon. This is done paying due attention to the shrinkage that characterizes the loss of moisture by a foodstuff. The resulting predictions of moisture loss and internal temperature change as a function of time are compared with experimental data. The sensitivity of the solution to the values of the transport properties is then tested.

CONCLUSIONS AND SIGNIFICANCE

It is shown that the model built provides acceptable predictions of moisture loss and internal temperature change with time, when shrinkage is taken into consideration. This is not the case when the predictions are made disregarding shrinkage. The sensitivity analysis indicates that the predictions change significantly when the effective mass diffusivity, heat transfer coefficient, or mass transfer coefficient are modified. They are much less sensitive to the values of effective thermal conductivity, heat of sorption and porosity.

The information obtained provides insight as to what is controlling the process from an internal and external standpoint. The structure of the subject matter should be helpful in designs and as a tool of innovation.

The equilibration of the water–foodstuff system involves a

Correspondence concerning this paper should be addressed to E. Rotstein.